

# X-RAY SPECTROSCOPY OF CATAclySMIC VARIABLES

Koji Mukai<sup>1</sup>

<sup>1</sup>*Code 662, NASA/Goddard Space Flight Center, Greenbelt, MD 20771, USA; also Universities Space Research Association*

## ABSTRACT

In cataclysmic variables (CVs), accretion onto white dwarfs produces high temperature, high density plasmas. They cool down from  $kT \sim 10$  keV via bremsstrahlung continuum and K and L shell line emissions. The small volume around white dwarfs means that the plasma densities are much higher than in, e.g., stellar coronae, probably beyond the range well-described by existing models. I will describe potential diagnostics of the temperatures, the densities, and the optical depths of X-ray emitting plasmas in CVs, and present the recent Chandra grating spectra of the magnetic CV V1223 Sgr as an example.

## MOTIVATION

Cataclysmic variables (CVs) are interacting binaries in which the accreting object (the primary) is a white dwarf (see Warner 1995 for a comprehensive review), unlike in X-ray binaries in which the accreting star is a neutron star or a black hole. CVs are numerous, as the following line of reasoning illustrates. In the Galaxy, there are about 35 classical novae per year (Shafter 1997). Since classical nova eruptions require the primary to have accreted  $\sim 1 \times 10^{-4} M_{\odot}$  of hydrogen-rich fuel, we infer the total accretion rate in CVs throughout our Galaxy to be about  $3.5 \times 10^{-3} M_{\odot} \text{ yr}^{-1}$ . If the mean accretion rate per CV is  $3.5 \times 10^{-10} M_{\odot} \text{ yr}^{-1}$ , then the total number of CVs in our Galaxy is about 10 million. Although such calculations are fraught with uncertainties, particularly in the mean accretion rate, and hence the total Galactic population may differ from this estimate by a factor of 10, there is no doubt that CVs are commonplace in our Galaxy. If we further assume a mean X-ray luminosity of CVs to be about  $4 \times 10^{31} \text{ ergs s}^{-1}$  (Mukai & Shiokawa 1993), the Galactic CVs might contribute  $\sim 4 \times 10^{38} \text{ ergs s}^{-1}$  of unresolved X-ray emission.

Moreover, the relatively high space density also means that the nearest members of the class are less than 100 pc from the Earth, close enough for detailed studies of the component stars and the accretion processes in many wavelength ranges: thus the CVs have proved to be an excellent laboratory for the study of accretion processes. Moreover, the relative shallowness of the potential well of a white dwarf means that the accretion disks of CVs are too cool to emit X-rays. Rather, CVs generate X-ray photons when material accretes onto the white dwarf. Because of the modest luminosities, these X-rays do not strongly influence the appearances of the accretion disks or alter the secular evolution of the systems. In many instances, therefore, we are able to study the accretion disk in the optical and in the UV, and the accretion process from the disk to the white dwarf in the X-rays, independent of each other. Such decoupling in CVs can be used to our advantage in understanding these systems, which can then be applied to a wider range of accretion powered X-ray sources.

## CV SUBCLASSES

Historically, optical astronomers have used the eruptive properties of CVs to classify them into dwarf novae, old novae, and nova-like systems. These are based on whether they have been seen to exhibit either of the two distinct types of outbursts known in CVs: dwarf nova outbursts, which are sudden brightenings of the accretion disk, and classical nova eruptions, which are thermonuclear runaways on the surface of the white dwarf. It is believed that dwarf nova outbursts are caused by an instability of the disk at a low

accretion rate; systems that accrete at a high rate, and systems without disks, do not show dwarf nova outbursts. It is likely that all CVs undergo classical nova eruptions once a sufficient amount of fresh fuel is accreted. This results in a typical recurrence time of  $>10,000$  years. Because high accretion rate systems with massive white dwarfs have the most frequent runaways, they therefore comprise the majority of old novae (=systems seen to undergo a classical nova eruption).

The X-ray properties of a CV is strongly influenced by the magnetic field of the primary, leading to an orthogonal scheme of CV subclassification. In Polars, or AM Her type systems, the primary is so magnetic (10 to  $>200$  MG) that no accretion disk can form, optical/infrared cyclotron emission is strongly detected, and the white dwarf spins synchronously with the binary orbit. The intermediate polars (IPs, or DQ Her type systems) are generally less magnetic, partial accretion disks are probably present, cyclotron emission is weak or undetected, and the white dwarf spin period is shorter than the orbital period. In both these subclasses, accretion proceeds quasi-radially along field lines onto the magnetic polar regions, and forms accretion “columns” or “curtains.” There a strong shock forms, heating the plasma to X-ray temperatures ( $kT > 10$  keV). The white dwarf surface below the shock is heated to  $kT \sim 20$  eV by these X-rays and by direct injection of kinetic energy by dense blobs. The IPs are the strongest source of 2–10 keV X-rays among CVs, with estimated luminosities in excess of  $10^{33}$  ergs  $s^{-1}$ , while the Polars are generally strong ( $\sim 10^{32}$  ergs  $s^{-1}$ ) soft X-ray sources.

Although less conspicuous to X-ray observers, the majority of CVs are the non-magnetic, low accretion rate dwarf novae. Dwarf novae in quiescence are relatively weak (a few times  $\sim 10^{31}$  ergs  $s^{-1}$ ) sources of medium energy X-rays. These X-rays are generated in a compact equatorial boundary layer between the disk and the white dwarf surface (see, e.g., Patterson and Raymond 1985a; Mukai et al 1997). There is no doubt that the material in the accretion disk just beyond the boundary layer has sufficient kinetic energy stored in its Keplerian motion to produce these X-rays. However, it is not clear exactly how the gas is heated to X-ray emitting temperatures. The very fact that medium energy X-rays are observed require that the emitting region is optically thin and the shocks are sufficiently strong (Pringle & Savonije 1979). Numerical solutions obtained by Narayan & Popham (1993) are consistent with such a picture; however, such studies to date suffer from a limited dimensionality and a dependence on the unknown viscosity parameter,  $\alpha$ . At higher accretion rates (dwarf novae in outburst, nova-like systems, and old novae), the boundary layer should become optically thick and radiate predominantly in the soft X-rays/EUV range (Patterson and Raymond 1985b). Although some systems do show the expected soft component, observations show that the high accretion rate systems also emit medium energy X-rays, perhaps from the optically thin surface of the boundary layer.

The magnetic CVs are better studied in X-rays than the non-magnetic systems, because they are brighter, and because the theory is more straightforward. I, too, will concentrate mostly on magnetic CVs in the rest of this paper, with occasional references to non-magnetic systems.

## X-RAY EMISSION FROM MAGNETIC CVS

### The Aizu Model

The Aizu model was originally developed for non-magnetic white dwarfs with a spherically symmetric accretion flow (Aizu 1973). However, its current applications are for magnetic CVs, which locally resemble the spherical case. In Aizu’s original paper, numerical solutions are given in the limit of small shock height,  $h$ . There are more modern treatments, either with different approximations, or with refinements: of the latter, the addition of a second cooling function (Wu et al 1994) representing cyclotron cooling is the most important. I will use the term “Aizu model” inclusively, including all these variations.

In the Aizu model for magnetic CVs, material follows the field lines to the surface, forming a strong shock. If the shock height is small, the shock temperature  $kT_s$  is determined by the white dwarf mass  $M_{wd}$ . For accreting material of solar abundances,  $kT_s \sim 21$  keV for  $M_{wd} = 0.6M_\odot$  and  $kT_s \sim 57$  keV for  $M_{wd} = 1.0M_\odot$ . The shock height in turn is determined by equating the settling time of the post-shock flow with its cooling time. Aizu assumed optically thin thermal bremsstrahlung to be the sole mechanism for cooling. Although Compton cooling probably is not relevant to most magnetic CVs (Frank et al 1983), we will return to the subject of an additional cooling mechanism in the next section.

In the Aizu model, the emergent X-ray spectrum is the sum of emissions from plasmas at different

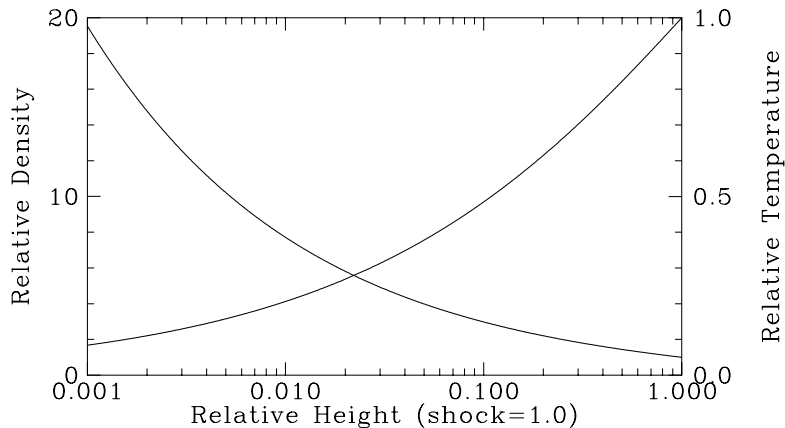


Fig. 1. The temperature and density profile in an Aizu shock, as function of height above the white dwarf surface. The relative temperature rises to the right, density to the left.

temperatures, from  $kT_s$  to the white dwarf photospheric temperature. As shown in Fig.1, the bulk of the post-shock region (note the logarithmic scale of the X axis) is hot and low-density. At an accretion rate per unit area of  $1 \text{ g cm}^{-2}\text{s}^{-1}$  onto a  $0.6M_\odot$  primary, the shock height is about 0.053 white dwarf radii ( $R_{wd}$ , or 460 km), and the density just below the shock is about  $1.0 \times 10^{16} \text{ cm}^{-3}$ . Thus, it is reasonable to ignore optical depth effects in modelling the X-ray continuum emission from just below the shock, as long as the accretion column radius is no more than, say, 500 km. Although the local accretion rate and the accretion column radius are both poorly known, these numbers can be considered typical: They result in a reasonable total luminosity, which is somewhat better constrained to be typically a few times  $10^{32} \text{ ergs s}^{-1}$  for Polars and a few times  $10^{33} \text{ ergs s}^{-1}$  for IPs.

### Simple X-ray spectral models

For low signal-to-noise, low spectral resolution spectra obtained with early X-ray satellite, however, a single temperature Bremsstrahlung model with a simple absorber was sufficient to fit the data. This was mostly the case in the 1970s, except that the need to include a reflection component was already seen in the HEAO-1 data on the prototype Polar, AM Her (Rothschild et al 1981). In magnetic CVs, a solid angle of  $\sim 2\pi$  steradians is subtended by the white dwarf surface, as seen from the post-shock plasma. Therefore, roughly half the original X-ray photons strike the surface, resulting in electron scattering, photoelectric absorption, and fluorescent line emission whose relative efficiencies are a strong function of the photon energy. This causes a characteristic bump in the continuum above 10 keV, as seen with HEAO-1, and the Fe  $K\alpha$  line at 6.4 keV. Indeed, emission line features in the 6–7 keV range are ubiquitous among magnetic CVs. However, in the proportional counter data, it was difficult to separate the contributions of the 6.4 keV reflection feature from those of thermal plasma at 6.7 keV (He-like Fe) and at 6.97 keV (H-like Fe).

Norton and Watson (1989) have presented their study of the spin modulation of IPs using EXOSAT data. They find that the spin modulation is stronger at lower energies, generally validating the “accretion curtain” model, in which the spin modulation is caused by photoelectric absorption in the accretion flow towards the magnetic poles. However, they also find that the energy dependence was not as strong as would be expected from pure photoelectric absorption. This suggests partial covering absorber: unfortunately, the statistics of the spin phase resolved spectra of magnetic CVs are usually not good enough to quantify this in detail, and one cannot distinguish spatial and temporal partial covering when analyzing phase-averaged spectra.

The Ginga LAC provided good data on magnetic CVs, often extending up to 30 keV. Using these, Ishida (1991) found typical Bremsstrahlung temperatures of  $\sim 15 \text{ keV}$  for Polars and  $\sim 30 \text{ keV}$  for IPs.

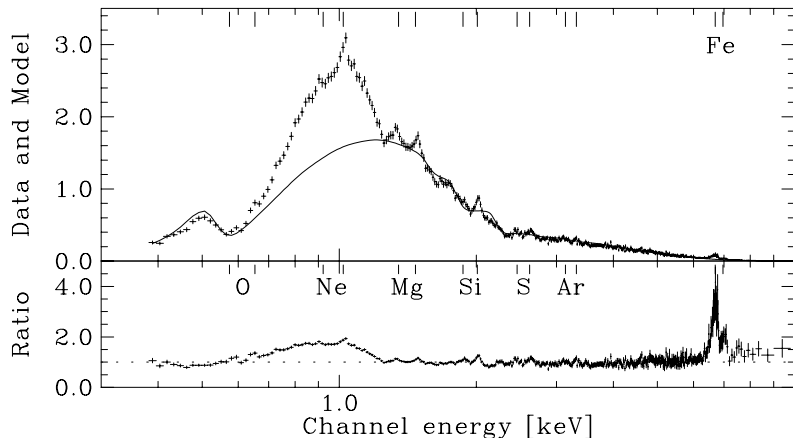


Fig. 2. The average ASCA SIS spectrum of the unusual IP, EX Hya. Thermal Bremsstrahlung plus absorber fit was performed to the data while ignoring the 0.7–1.2 keV region. The top panel shows the data with this best-fit Bremsstrahlung model; the bottom panel shows the ratio of data to the model. Energies of H-like and He-like  $K\alpha$  lines of O, Ne, Mg, Si, S, Ar and Fe are shown. The spectrum is clearly dominated by the Fe L complex around 1 keV.

### Thermal lines from the post-shock plasma

Ishida et al (1994) observed the unusual IP, EX Hya, with the ASCA SIS. In addition to the Fe  $K\alpha$  lines, they discovered  $K\alpha$  lines of Ne, Mg, Si, S, and Ar for the first time, directly establishing the presence of multi-temperature plasma in this system (see Fig.2). Moreover, something about the temperature distribution can be inferred from the line ratios: in fact, Fujimoto and Ishida (1997) have converted these into the shock temperature, and estimated the primary of EX Hya to be  $0.48 M_{\odot}$ . They also infer the temperature at “the bottom of the shock” to be  $\sim 0.65$  keV, yet do not discuss the fact that the true photospheric temperature must be much lower in this system (the EUVE spectrum extends to  $\sim 180\text{\AA}$ , without showing any signs of the soft, blackbody-like component; see Hurwitz et al 1997). The Fe  $K\alpha$  lines in EX Hya are resolved into 3 components, although the 6.4 keV line is rather weak in this system. Finally, the spectrum of EX Hya around 1 keV is dominated by the Fe L features, which is a characteristic of thermal plasma with  $kT \sim 1$  keV.

The strength of the Fe L complex in EX Hya (also seen in the X-ray spectrum of stellar coronae) points out an inadequacy of the Aizu model: the assumption of the Bremsstrahlung cooling breaks down for optically thin,  $kT \sim 1$  keV plasma. Such a plasma cools, instead, predominantly by emitting Fe L photons (see, e.g., Gehrels and Williams 1993). Thus, the Aizu model overestimates the cooling time appropriate for the  $kT \sim 1$  keV region, and overestimates its height. More importantly, integrating plasma emission models over the emission measure distribution calculated using the Aizu model would result in a significant overprediction of the Fe L feature in magnetic CVs.

However, this turns out to be the least of problems, when applied to most magnetic CVs other than EX Hya. Among ASCA archival spectra of magnetic CVs, strong Fe L features are the exception, not the rule. The case for this is particularly strong for the typical IP, V1223 Sgr (Fig.3). Even though the continuum is strongly detected down to  $\sim 0.4$  keV, there is no sign of the Fe L features. This, therefore, cannot be explained as due to photoelectric absorption (which would remove continuum and line photons equally; any photoelectric absorption which removes the Fe L photons will not let  $\sim 0.4$  keV continuum photons through), and points to a real problem in applying the standard spectral model to real magnetic CVs. Of the 20 or so magnetic CVs observed with ASCA, only EX Hya, YY Dra, V884 Her, and AE Aqr show strong Fe L features. Similarly, many magnetic CVs show only weak evidence for  $K\alpha$  lines of elements other than Fe. Several lines of arguments suggest that EX Hya has an exceptionally low accretion rate for an IP, and hence a relatively tall, low density shock; this may be somehow connected to the ease with which low energy lines have been detected in this system.

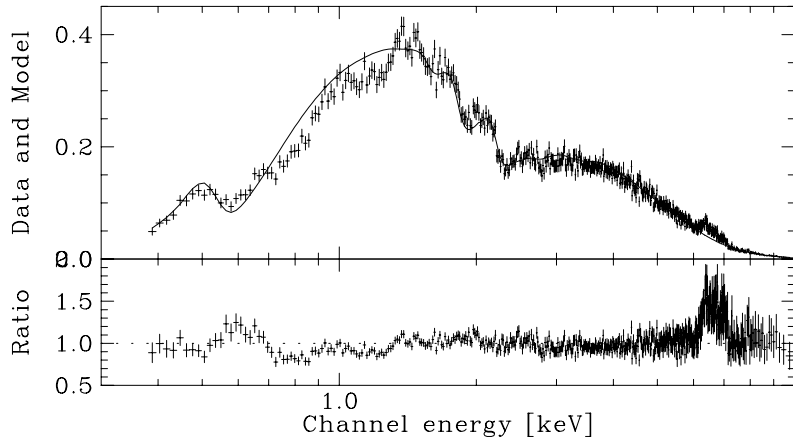


Fig. 3. Same as Fig.2, but for V1223 Sgr. A strong Fe L bump seen in EX Hya is absent in this system.

A similar situation exists for non-magnetic CVs. They, too, should exhibit multi-temperature plasma emission. There are several cases where strong Fe K and L features are seen (e.g., V603 Aql), which is a direct evidence for at least two temperature components; there are other cases where the Fe L features are absent (e.g., HT Cas). For both non-magnetic and magnetic CVs, it is highly unlikely that an X-ray emitting plasma can cool to white dwarf photospheric temperatures without emitting Fe L photons. Rather, we may try to modify the standard model by considering a geometry in which the lower temperature component is selectively hidden, while allowing the higher temperature component (which also emits low energy continuum photons) to escape.

The study of Fe  $K\alpha$  lines have turned out to be more fruitful: the fluorescent component can often be separated from the thermal components, and evidence has been found for a significant broadening of the thermal lines in some systems, while they appear narrow in others (Hellier et al 1998). For example, the 6.4 keV line in the IP AO Psc appears narrow, while the thermal lines are blended into a broad bump; in contrast, V1223 Sgr (which is otherwise very similar to AO Psc) appears to have three narrow Fe  $K\alpha$  lines in the ASCA data. Having considered, and discarded, several possibilities such as bulk Doppler motion, Hellier et al consider Compton scattering to be the most likely broadening mechanism. If the opacity for the thermal line core is high enough, line photons will be trapped, and they can only escape after Compton scattering, which degrades the photon energy. The possibility that resonant scattering in the post-shock region can also enhance the equivalent width of the Fe  $K\alpha$  feature, when viewed along the magnetic axis, has been discussed by Terada et al (1999). The true test of this attractive idea would be a phase-resolved observation of a system whose geometry is established from other means. Similarly, better data as well as more detailed calculations are required to test if the resonant trapping/Compton scattering mechanism can quantitatively explain the broadened line profiles.

### PRE-SHOCK FLOW

If the shock height is small, then a substantial fraction of the X-rays emitted in the post-shock region must traverse the pre-shock flow.

### Absorption Effects

As already mentioned, Norton and Watson (1989) discovered that partial-covering absorption was necessary to model the spectrum of IPs. The true complexity of the intrinsic absorption is revealed by the following exercise, divised by Osborne (1994, private communication). In this, one fits a simple (Bremsstrahlung plus a single, cold, absorber) model to the ASCA spectrum of a magnetic CV, first in the entire ASCA range ( $\sim 0.4$ – $10$  keV). Next, raise the lower limit of energy range to 1.0, 2.0, 3.0, etc. keV and repeat the fit. One finds that the best fit kT and  $N_H$  values change as a function of the lower limit, revealing that the observed spectrum cannot be adequately modeled by a simple absorber.

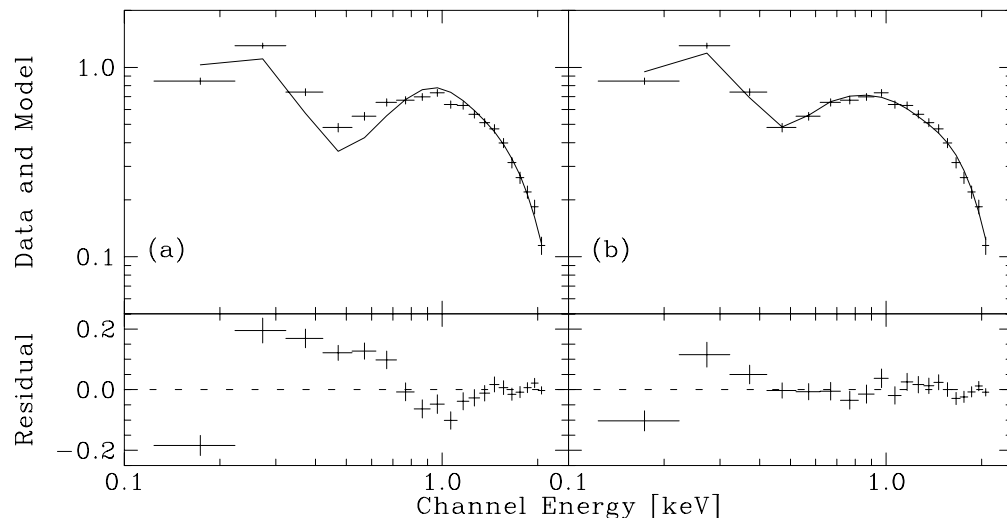


Fig. 4. A ROSAT PSPC spectrum of V1223 Sgr, shown twice with different model fits. (a) Fitted with a partial-covering absorber model; (b) Fitted with an ionized absorber model. The smaller residuals for the latter suggests the presence of an ionized absorber in this system, but the residuals can also be reduced by introducing a second cold partial-covering absorber.

This is not surprising: the lines-of-sight to different parts of the post-shock gas pass through different amounts of pre-shock flow. One can generalize the partial covering absorber model to, say, a power-law distribution of  $N_H$  (Done and Magdziarz 1998). Unfortunately, even this is a phenomenological model; unless we can determine the complex geometry of the accretion flow, one cannot create a realistic model of the complex absorption.

Moreover, the pre-shock flow should be ionized. The degree of ionization is, again, geometry-dependent: the pre-shock flow is less ionized if more radiation can escape from the sides of the post-shock region. If little radiation can escape from the sides (if accretion column radius is much larger than the shock height, this would be the case just above the shock), the ionization parameter  $\xi$  can be several hundred. Indeed, ASCA and ROSAT spectra of several magnetic CVs do suggest the presence of warm absorbers, but do not uniquely prove it: an alternative fit involving multiple partial covering absorber can usually be found (see, e.g., Fig. 4). To reach a final conclusion on this issue, one would need to attempt a direct detection of warm absorber edges in higher spectral resolution, high signal-to-noise spectra.

### Scattering and re-emission

However, absorption is not the only physical process that takes place in the pre-shock flow. Some electron scattering will take place, particularly if the plasma is significantly ionized; also, photoelectric absorption will be followed by continuum and/or line emission at lower energies. Because the geometry of the pre-shock flow is far from spherically symmetric around the emission region, the relative importance of absorption vs. emission depends strongly on the viewing geometry, which in turn depends on the binary inclination angle and the spin phase.

In most magnetic CVs, the case for photoionized plasma emission has been ambiguous. For example, Kallman et al (1993) included such a component in their interpretation of the BBXRT spectrum of BY Cam. However, Done and Magdziarz (1998) consider that low energy features in this system, seen with ASCA, are due to thermal emission from multi-temperature plasma. The best case so far of photoionized plasma emission may be found in the spin minimum of AM Her: although the predominant magnetic pole is hidden behind the white dwarf limb at this phase, a weak X-ray source remains in view (Ishida et al 1997). The pre-shock flow is a plausible origin of this component. However, emission from the second pole cannot be excluded.

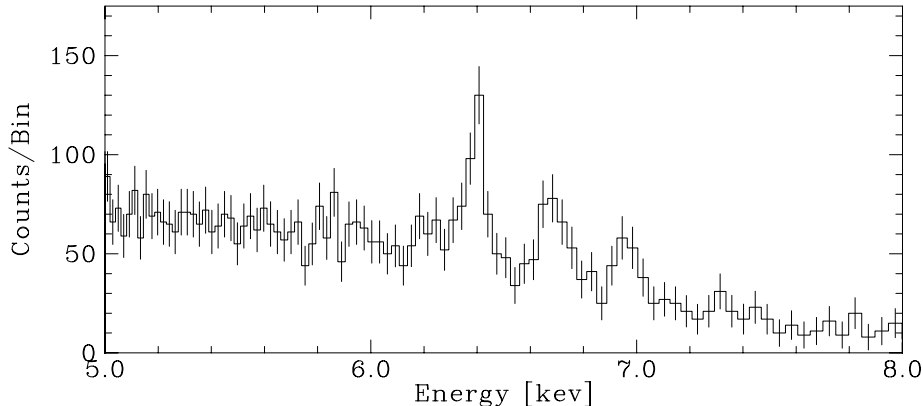


Fig. 5. The average Chandra HETG (HEG) spectrum of V1223 Sgr in the 5–8 keV range. The Fe  $K\alpha$  feature is clearly resolved into three, narrow, components. In addition, the 6.4 keV (fluorescent) component may have a shoulder extending to  $\sim 6.2$  keV.

### CHANDRA HETG OBSERVATION OF V1223 SGR

In previous sections, I have reviewed the state of the art in X-ray spectroscopy of (mostly magnetic) CVs in 1999. Although many recent data (notably those obtained with ASCA and BeppoSAX) remain to be exploited fully, there are several important questions that require higher resolution data. Perhaps the instrument that would have best matched the scientific objectives was the XRS on-board ASTRO-E; nevertheless, grating instruments on XMM-Newton and Chandra both have the potential to advance our knowledge of CV X-ray spectra significantly. In the rest of this article, I will describe preliminary results from a Chandra HETG observation of X-ray bright IP, V1223 Sgr, obtained on 2000 April 30/May 1 for approximately 52 ksec. Analysis and interpretation of the data are still ongoing.

First, the Fe  $K\alpha$  feature of this system clearly consists of 3 separate components (see Fig. 5). The detected line widths for the 6.7 and 6.97 keV thermal lines appear consistent with instrumental resolution, confirming the ASCA result. Thus, V1223 Sgr should serve as a baseline; a Chandra HETG observation of AO Psc, the system for which the line broadening is most securely detected in ASCA data, is scheduled in Cycle 2.

The 6.4 keV (fluorescent) component also largely appears to be narrow, however a shoulder, extending down to  $\sim 6.2$  keV, is tentatively detected. This might indicate that some 6.4 keV line photons (but not the thermal line photons) suffer Compton degradation. Alternatively, some of the fluorescence line may originate in the pre-shock flow, which may have sufficient bulk velocity to Doppler shift the line energy by up to  $\sim 200$  eV.

The MEG data (Fig.6) reveal a rich emission-line spectrum, comparable to that of EX Hya observed with the ASCA SIS. Lines are detected from H- and He-like ions of O, Ne, Mg, Si, S, and probably Ar. Moreover, the MEG resolves the resonant, intercombination, and forbidden triplets from He-like ions of O, Ne, and Mg. The forbidden lines are very weak, suggesting relatively high density, and the intercombination lines are comparable to the resonant components, suggesting photoionization origin. Moreover, we do not detect strong Fe L features; their weakness is another evidence for photoionization origin. Finally, when plotted in 10 eV bins, the presence of the OVII warm-absorber edge at 0.739 keV is strongly suggested.

It is therefore likely that these features originate in the immediate pre-shock flow. The only other body near the emission region, the white dwarf itself, has a much higher density and therefore a lower ionization parameter value than is required to produce these features. As we have already speculated, the pre-shock flow on the other hand is a natural origin both for the warm absorber and of the photoionized plasma emission. Detailed analyses are in progress to quantify the conditions of the pre-shock flow using these new diagnostics opened up by the Chandra grating instrument.

We are left with a major question, however: Where are the expected thermal lines from the post-shock,

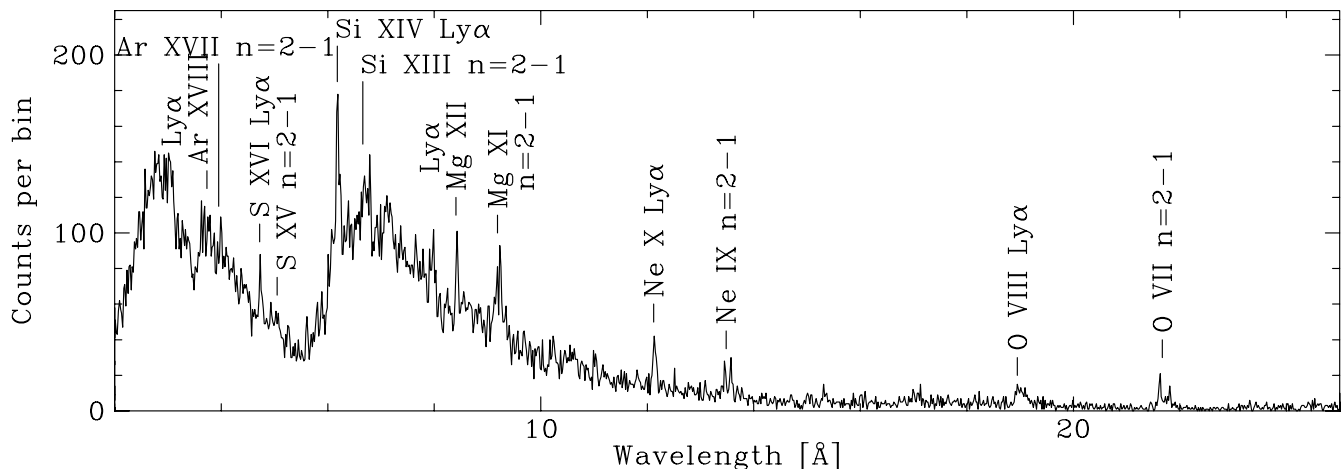


Fig. 6. The Chandra HETG (MEG) spectrum of V1223 Sgr, plotted against wavelength.

cooling plasma? The presence of a strong Fe L bump in the ASCA spectrum of EX Hya, among other clues, suggests that it is the lines from coronal plasma that we have detected with the SIS. Analyses of Chandra and XMM-Newton grating observations of this system are expected to confirm this interpretation. Even though similar K shell features are seen, V1223 Sgr appears completely different in this respect. Comparison of ASCA spectra suggest that V1223 Sgr is more typical of magnetic CVs, whereas EX Hya belongs to a smaller group perhaps with 3 other systems, characterized perhaps by low accretion rates.

One possible explanation for the difference between the two magnetic CVs (perhaps two groups of magnetic CVs) is the following. In the Aizu model, the plasma density increases sharply towards the bottom of the shock. Eventually, the post-shock region becomes optically thick in the continuum. In EX Hya, this happens at about 0.65 keV, as suggested by the analysis of Fujimoto and Ishida (1997), while in V1223 Sgr, this happens at a much higher temperature, say  $kT \sim 2$  keV as has been suggested by Beardmore et al (2000). Earlier works calculated the optical depth across the accretion column just below the shock; their conclusion that that region is optically thin remains valid. However, most of the observed medium energy (0.5–10 keV) X-rays actually originate much lower down in the post-shock region (Fig.7). For example, this plot shows that, for a  $kT_s = 20$  keV shock, we need to use  $E \sim 40$  keV continuum photons to probe the upper, low-density part of the post-shock region. Most of the photons we observe with ASCA, for example, must come from the bottom  $\sim 1\%$  of the shock! The situation is more extreme for low energy line photons: the emissivity of  $K\alpha$  lines of elements up to Si and S, as well as those of the Fe L lines, peaks at temperatures below 2 keV in a collisionally ionized plasma. In an Aizu shock with  $kT_s = 20$  keV, this is the bottom  $\sim 0.1\%$  of the shock, where the density is  $\sim 20$  times greater than immediately below the shock.

These line photons cannot escape freely by travelling vertically, either, partly because of the photoelectric absorption in the cool, pre-shock, flow. Moreover, the vertical electron scattering optical depth within the post-shock region is non-negligible: the characteristic cooling time of the post-shock plasma is inversely proportional to the local accretion rate, and is  $\sim 1$  s at  $1 \text{ g cm}^{-2} \text{ s}^{-1}$ . Thus we expect  $\sim 1 \text{ g cm}^{-2}$  of vertical column in the post-shock region; in fact, a numerical integration which properly accounts for the deceleration shows that the actual number is  $\sim 2 \text{ g cm}^{-2}$ , with a weak dependence on the primary mass. It therefore appears that most of the low energy line photons from the bottom can be hidden by a significant optical depth; exactly how this works depends on the shock geometry. In addition, the white dwarf atmosphere has a scale height of several kilometers, when heated to  $kT \sim 20$  eV (this applies only to the area surrounding the accretion column; underneath the column, the ram pressure will reduce the scale height). Thus, there may be a puffed up ring of white dwarf atmosphere, further reducing our ability to see the low energy line emissions. Thermal Fe  $K\alpha$  lines, which come from higher up in the post-shock region, is probably



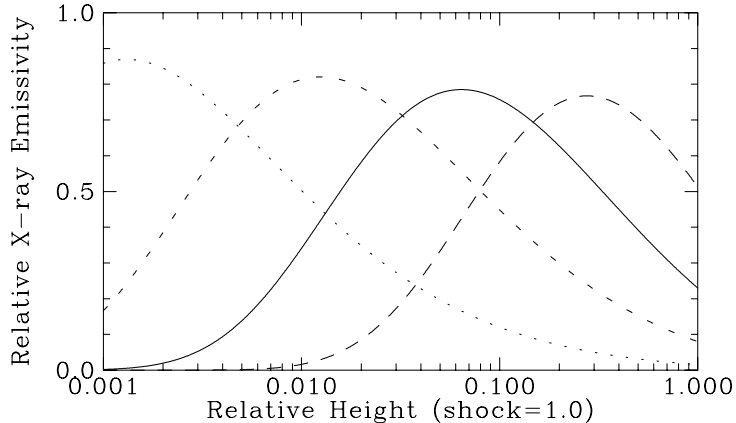


Fig. 7. The relative emissivity of  $E=2kT_s$  (long dashes),  $1.0kT_s$  (solid),  $0.5kT_s$  (medium dashes), and  $0.2kT_s$  (short dashes) continuum photons as a function of shock height in an Aizu model.

responsible for the 6.7 and 6.97 keV features seen in V1223 Sgr. The shock models would suggest that the Fe  $K\alpha$  emitting region is optically thin in the continuum. This is consistent with the Hellier et al. (1998) interpretation of the broad Fe  $K\alpha$  lines, which requires a continuum optical depth of 0.05–1.0 in the line emitting region, where the temperature is  $kT \sim 5$  keV.

The accretion rate also controls the efficiency of pre-shock flow heating. Low accretion rate shocks are so tall that most of the radiation escapes from the side, lowering the degree of photoionization just above the shock. Thus, EX Hya could have very little emission lines from this region while V1223 Sgr is dominated by it.

## CONCLUSIONS SO FAR AND FUTURE PROSPECTS

The Aizu shock model attempts to connect the optically thick region immediately below the shock to the extremely optically thick white dwarf atmosphere. With hindsight, it is therefore natural that optical depth plays a significant role in shaping the observed X-ray spectra of magnetic CVs. It appears that the low energy X-ray line features of V1223 Sgr and EX Hya have different origins, despite some superficial similarities. There is evidence that the low energy lines seen in V1223 Sgr are from a dense, photoionized plasma, probably in the pre-shock flow. The lines in EX Hya are from the cooling post-shock plasma; these are weaker or hidden in V1223 Sgr. It is still likely that the Fe  $K\alpha$  lines share the same origins (fluorescence off the white dwarf surface for the 6.4 keV line, thermal plasma emission for the other two components), since photoionization is unlikely to be strong enough to produce a significant Fe  $K\alpha$  feature in any CVs. It has been suggested that resonant trapping of these line photons is the cause for the broadening of these thermal Fe  $K\alpha$  lines in some systems; We await the recently approved Chandra grating observation of AO Psc to explore the details of this mechanism. Along with more observations, a more detailed modelling is also necessary. However, if optical depth does play an important role in shaping the X-ray spectrum, as I have argued in this paper, then a realistic geometry must be used in numerical simulations. Therefore, it appears essential to improve our knowledge of the detailed shape of the post-shock region through, e.g., the observations of eclipses and self-occultations of the X-ray emitting region.

What can we expect for non-magnetic CVs? Despite the differences in geometry, X-ray emitting regions in magnetic and non-magnetic systems share some essential features: boundary layer emission in the latter must originate in a shock-heated plasma which cools down, and becomes denser, before it can settle down onto the primary surface. The depth of the gravitational potential, the size of the emitting region, and the local accretion rate are all similar between magnetic and non-magnetic CVs. Therefore, it is possible that the optical depth effects become important below some critical temperature, hiding any intrinsic line features, in non-magnetic as well as in magnetic systems. With future high quality X-ray spectra, we may

begin to detect broadened lines, warm absorbers, and photoionized plasma emissions in non-magnetic CVs, a very exciting prospect indeed.

## ACKNOWLEDGEMENTS

I thank Chris Done and Coel Hellier for their critical reading of this manuscript. I also thank Manabu Ishida, and Tim Kallman for the insights that they have shared with me over the years.

## REFERENCES

- Aizu, K., X-ray Emission Region of a White Dwarf with Accretion, *Prog. Theor. Phys.*, **49**, 1184, 1973.
- Beardmore, A.P., Osborne, J.P, and Hellier, C., The multi-temperature X-ray spectrum of the intermediate polar V1223 Sagittarii, *MNRAS*, **315**, 307.
- Done, C., and Magdziarz, P., Complex absorption and reflection of a multitemperature cyclotron-bremsstrahlung X-ray cooling shock in BY Cam, *MNRAS*, **298**, 737, 1998.
- Frank, J., King, A.R., and Lasota, J.P., Column accretion on to white dwarfs, *MNRAS*, **202**, 183, 1983.
- Fujimoto, R., and Ishida, M., X-ray spectroscopic observations of EX Hydrae and mass determination of the white dwarf, *ApJ*, **474**, 774, 1997.
- Gehrels, N., and Williams, E.D., Temperatures of Enhanced Stability in Hot Thin Plasmas, *ApJLett*, **418**, L25, 1993.
- Hellier, C., Mukai, K., and Osborne, J.P., Iron K $\alpha$  line widths in magnetic cataclysmic variables, *MNRAS*, **297**, 526, 1998.
- Hurwitz, M., Sirk, M., Bowyer, S., and Ko, Y.-K., EUV observations of EX Hydrae: 10<sup>7</sup>K gas near a white dwarf surface, *ApJ*, **477**, 390, 1997.
- Ishida, M., X-ray Observations of Accreting Magnetic White Dwarfs, PhD Thesis, University of Tokyo, 1991.
- Ishida, M., Matsuzaki, K., Fujimoto, R., Mukai, K., and Osborne, J.P., Detailed X-ray spectroscopy of AM Herculis with ASCA, *MNRAS*, **287**, 651, 1997.
- Kallman, T.R., Schlegel, E.M., Serlemitsos, P.J., Petre, R., Marshall, F., Jahoda, K., Boldt, E.A., Holt, S.S., Musthozky, R.F., Swank, J., Szymkowiak, A.E., Kelley, R.L., Smale, A., Arnaud, K., Weaver, K., and Paerels, F.B., Broad-band X-ray telescope observations of the magnetic cataclysmic variable H0538+608 = BY Camelopardalis, *ApJ*, **411**, 869, 1993.
- Kallman, T.R., Liedahl, D., Osterheld, A., Goldstein, W., and Kahn, S., Photoionization Equilibrium Modelling of Iron L Line Emission, *ApJ*, **465**, 994, 1996.
- Mukai, K., and Shiokawa, K., The EXOSAT Medium Energy (ME) Sample of Dwarf Novae, *ApJ*, **418**, 863, 1993.
- Mukai, K., Woods, J.H., Naylor, T., Schlegel, E.M., and Swank, J.H., The X-ray eclipse of the dwarf nova HT Cassiopeiae: Results from ASCA and ROSAT HRI observations, *ApJ*, **475**, 812, 1997.
- Narayan, R., and Popham, R., Hard X-rays from accretion disk boundary layers, *Nature*, **362**, 820, 1993.
- Norton, A.J., and Watson, M.G., Spin modulated X-ray emission from intermediate polars, *MNRAS*, **237**, 853, 1989.
- Patterson, J., and Raymond, J.C., X-ray Emission from Cataclysmic Variables with Accretion Disks. I. Hard X-rays, *ApJ*, **292**, 535, 1985a.
- Patterson, J., and Raymond, J.C., X-ray Emission from Cataclysmic Variables with Accretion Disks. II. EUV/Sard X-ray Radiation, *ApJ*, **292**, 550, 1985b.
- Pringle, J.E., and Savonije, G.J., X-ray emission from dwarf novae, *MNRAS*, **187**, 777, 1979.
- Rothschild, R.E., Gruber, D.E., Knight, F.K., Matteson, J.L., Nolan, P.L., Swank, J.H., Holt, S.S., Serlemitsos, P.J., Mason, K.O., and Tuohy, I.R., The X-ray spectrum of AM Herculis from 0.1 to 150 keV, *ApJ*, **250**, 723, 1981.
- Shafter, A.W., On the Nova Rate in the Galaxy, *ApJ*, **487**, 226, 1997.
- Warner, B., Cataclysmic Variable Stars, Cambridge University Press, Cambridge, 1995.
- Wu, K., Chanmugam, G., and Shaviv, G., Structure of steady state accretion shocks with several cooling functions: Closed integral-form solution, *ApJ*, **426**, 664, 1994.